RiESTech

Recent in Engineering Science and Technology

MBI

Article

Effect of Rheological on the Physical and Electrical Properties of Extruded Micro Carbon-LLDPE Composites

Aminudin Zuhri [1], Agus Edy Pramono [1,*], Iman Setyadi [1], Nanik Indayaningsih [2]

[1] Magister Program in Applied Manufacturing Technology Engineering, Politeknik Negeri Jakarta, Jl. 440-442, Tangerang Selatan, BantenI, Depok 16425, Jawa Barat, Indonesia
[2] Research Center for Advanced Material, National Research, and Innovation Agency (BRIN), Kawasan Puspiptek, Gd. 440-442, Tangerang Selatan, Banten 15310, Indonesia
* Correspondence: agus.edypramono@mesin.pnj.ac.id

Abstract: This study focuses on formulating and optimizing a conductive polymer composite (CPC) material tailored for electromechanical applications. Linear Low-Density Polyethylene (LLDPE) polymer and micro carbon particles derived from rice husk were compounded using a hot compaction process and melt blended through a single-screw extrusion machine. A mix of 50% loading of microcarbon particles was used in this research. It was determined that the experiment was successfully conducted, resulting in a stabilized density of approximately 1 g/cm^3. The research demonstrates how the prototype Extruder Head effectively stabilizes the density of composites. Electrical conductivity demonstrated a notable increase in conductivity toward higher density. These findings underscore the successful development of a CPC material with improved electrical conductivity, making it a highly suitable tool for high carbon-loading composite material.

Keywords: Carbon-LLDPE Composite; Rice Husk Carbon; Electrical Conductivity; Conductive Carbon; Extruder Head

Citation:. Zuhri, A., Pramono, A. E., Setyadi, I., Indayaningsih, N. (2024). Effect of Rheological on the Physical and Electrical Properties of Extruded Micro Carbon-LLDPE Composites. Recent in Engineering Science and Technology, 2(04), 23–33. Retrieved from https://www.mbi-journals.com/index.php/riestech/article/view/77

Academic Editor: Vika Rizkia

Received: 17 August 2024
Accepted: 16 October 2024
Published: 31 Ocotber 2024

1. Introduction

This article discusses the engineering development of filament materials for 3D Printing/3DP applications using CPC materials. Carbon polymer composites are also called CPC due to the conductive properties perceived in the composites that are fundamentally influenced by the van der Waals forces between the fillers. These forces maintain a complex network of fillers within the composite during filament manufacturing [1]. Polymer materials can be engineered into composite materials by adding reinforcing agents/fillers to enhance their mechanical, thermal, electrical/magnetic, and chemical properties. Carbon materials have been widely used as filler materials in 3DP for various applications, from medical to energy storage [2]. The melt blending process is commonly used in compounding in filament manufacturing [3]. In this process, shear energy is harnessed by the rotation of the extrusion machine's screw, which is particularly effective when employing twin-screw extruders [3]. However, single-screw extrusion machines [4] can produce 3DP filaments using the master batch dilution method [3]. These machines can also be utilized for direct low-carbon concentration composites [5]. It is important to note that manufacturing filaments with high filler concentrations cannot be achieved using single-screw extrusion machines [5]. Generally, CPC production aims to achieve a low percolation threshold [3]. However, this article takes a contrary approach [2] —the melt blending method benefits nano-sized fillers, achieving percolation thresholds at low concentrations. However, high filler concentrations do not significantly enhance electrical conductivity values in advancements [6]. In the case of using micro-sized carbon filler, higher concentrations are needed to reach the percolation threshold, thus requiring increased amounts of carbon [7]. Auxiliary tools supporting the extrusion process include the extruder head [8] equipped with spider legs [9]. It is suspected that these auxiliary tools can transform the turbulent fluid flow of composites with high carbon concentrations into the laminar fluid flow, affecting the rheological properties of the composite within the extruder head chamber [10]. The article explores experiments on producing high-carbon content polymer composites with loading up to 50%, a fraction not mentioned in the referenced journal article [11]. Experiments used micro-sized carbon from organic rice husks to investigate how stabilizing density affects electrical conductivity in the extruder head chamber.

2. Materials and Experiment Methods

The fabricated carbon filler is powdered with a particle size of micro mesh #200 and a density of 1.4 g/cm³ [2]. The virgin polymer used #40 mesh and a 0.91-0.98 g/cm³ density of ETILINAS LL3840UA [7]. The design of the tools [9] was created using the Solidwork/SW simulator [2], and the design of the spider leg can be seen in Figure 3. The melt blending process was carried out using a single-screw extrusion machine with an L/D Screw ratio of 19 [12]. The spider leg was fabricated using conventional machinery, and the assembly of the tools [2] can be observed in Figure 2.

The 3D printing filament was manufactured with a composition of polymer to micro carbon at a loading ratio of 50:50. The machine was heated with the motor running until each zone reached its temperature: 200°C for Zone 1, 150°C for Zones 2 and 3, and 110°C for the Extruder Head. The Extruder head was divided into four zones for density characterization based on geometric changes illustrated in Figure 1.

Comparison experiment: composites fabricated via hot compaction molding at 130°C with a holding phase at 115°C, applying 100 bar compaction pressure on it at the same composition. Density testing was conducted according to ASTM D792 standards [13, 14, 15]. Electrical conductivity was tested using the two-contact probe/TCP method [16].

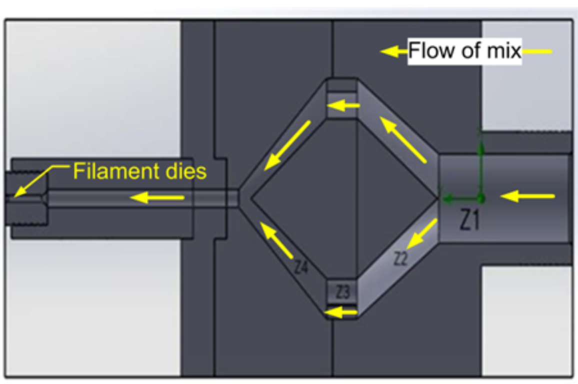

Figure 1. Affected Zone in Extruder Head Chamber

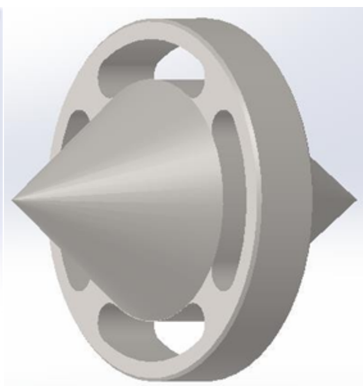

Figure 2. Designated Spider L

Microstructure observations were carried out using Scanning Electron Microscopy/SEM with a Hitachi SU3500 machine at the National Research and Innovation Agency/BRIN laboratory, equipped with elemental analysis through SEM-EDX (Energy Dispersive X-ray) [17].

3. Results and Discussion

3. 1 Composite Density in zones

The experiment used a primary extrusion machine to extrude a composite material containing a 50% loading of microcarbon from rice husks mixed with LLDPE. Experiments conducted with an extruder head demonstrated a stable composite density within the extruder head zones [2]. The composite material was extruded from the nozzle and then molded through a hot compaction process, yielding samples with a density of approximately 1 g/cm³.

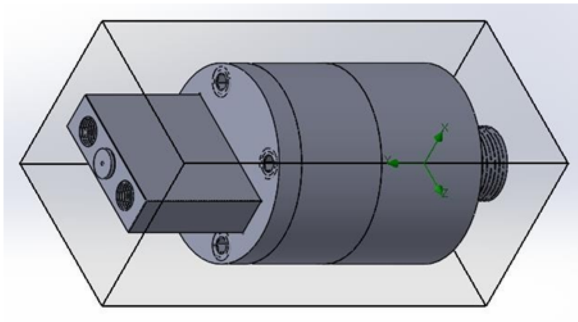

Figure 3. Extruder Head Assembly

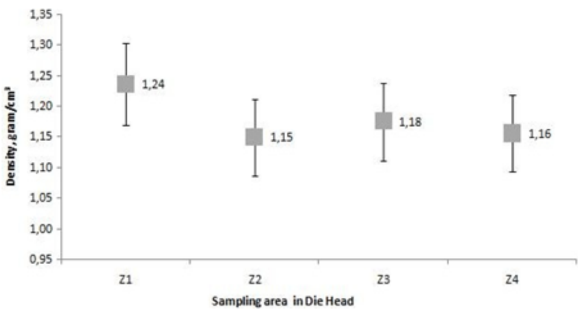

Figure 4. Density of Composite at the Extruder Head Zone

Microstructure analysis of composite material in Z3 confirmed the effective dispersion of micro carbon from rice husks in this relaxation zone. The density increase in Z3 indicated an efficient function of the spider leg. Rapid compression flow from Z1 filled up Z2 before rising in Z3. Composite flow converged towards a standard exit between spider legs, with no abnormal carbon concentrations detected (confirmed data shown in Figure 4). SEM imaging at 100× Magnification revealed a lot of stacked layers of carbon-rich matrix.

3. 2 Microstructure of rheological and elements

At 500× Magnification, numerous voids were observed in the microstructure, commonly encountered in composite manufacturing, indicating compounding challenges [6]. High-contrast areas, representing grain boundaries, show high carbon concentration at interphase areas. Despite filler particles being micro-scale, significant energy is required for polymer-composite interaction. Composite formation disrupts the aggregation of micro-scale carbon particles via adsorption, but nano-scale carbon particles aggregate quickly, leading to void formation.

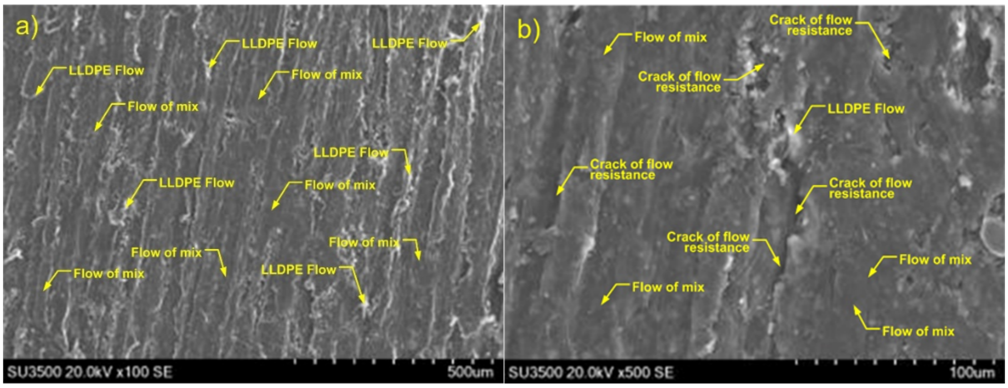

Figure 5. Microstructure at Z3 Chamber, Fluid Pattern Structure

a) at 100×; b) at 500×Magnification

The carbon-rich areas are uniformly dispersed, as observed in SEM images in Figure 5a. This condition does not become apparent in experiments utilizing the hot compaction technique. There are no discernible carbon-rich layers, as depicted in Figure 6. The carbon-rich layers show random circular boundaries without directional flow patterns; notable differences in these layers are evident in samples made via hot compaction methods. The initial composition before the molding process had been manually controlled using the same compounding method. There are conjectures of possible alterations in the carbon composition during the molding process by extrusion and hot compaction.

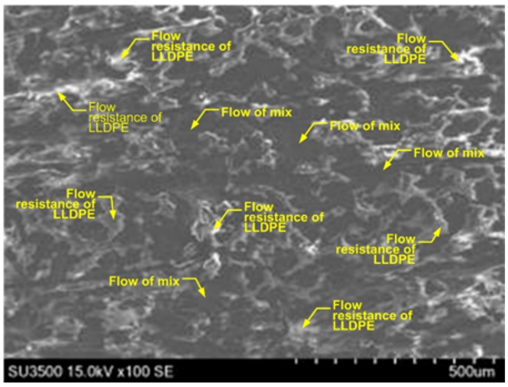

Figure 6. Micro Structure of flow resistance of composite

Elemental testing with the SEM EDX method did not generally reveal significant differences in carbon elements. Table 1 depicts the percentage data of the main elements in the composite, its values resembling each other. Otherwise, it can still be deduced that both composite samples' compositions remained unchanged during molding. Analyzing the SEM EDX data alongside SEM microstructure observations suggests that there is a decrease in the proportion of carbon-rich layers within the composite samples extruded using the extrusion machine. The carbon that forms the polymer chain in LLDPE has the highest composition [18] because polymers are essentially composed of hydrocarbons.

SEM EDX selective observation reveals silica elements acting as impurities within the microcarbon in the microstructure observation area, as shown in Table 2 [19]. An analysis of micro carbon alteration composition can be carried out using two composite molding methods. In Figure 7a, a sample point is shown at the grain boundary area of microcarbon particles from rice husks, and in Figure 7b, a sample point is displayed on silica particles.

Table 1. Main Elements in Spectrum 1

Element	% wt	
	Extrusion	Compaction
C	87,25	82,23
O	7,44	12,74
Si	4,63	3,5

Table 2. Main Elements in Spectrum 2

Element	% wt	
	Spectrum 1	Spectrum 2
C	52,06	8,37
O	17,61	51,03
Si	14,08	40,60

Referring to these two sets of imaging data, it can be inferred that the dispersion of rice husk microcarbon is entirely satisfactory within the observation area. Note that samples in Figure 7 are extruded using extruder head tools. Figure 8 compares observations of composite samples molded via hot compaction and extrusion methods. The interphase area of the extruded composite sample is significantly reduced.

Figure 8 also shows the features suspected to be plastic flow resistance of the LLDPE matrix during the molding process, as shown in Figure 8 (a). Likewise, Figure 8 (b) shows crack features, indicating the suspected occurrence of rheological flow resistance from LLDPE plastics by accompanying carbon particles.

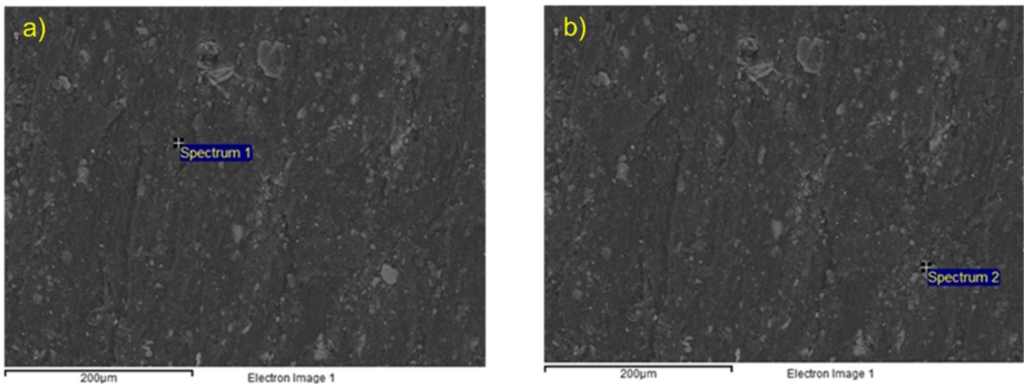

Figure 7. Micro Structure of Micro Carbon Particle Derived from Rice Husk at 250× Magnification observed from a) Particle Spectrum 1 and b) Particle Spectrum 2 Sampling

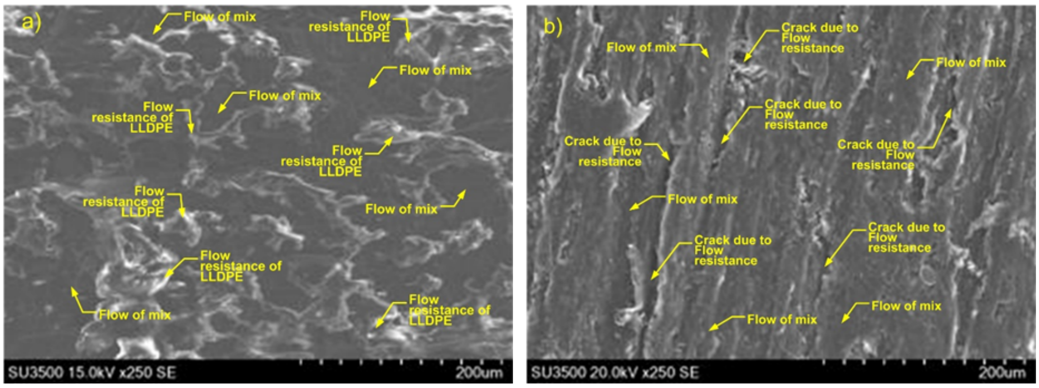

Figure 8. Micro Structure Observed at 250× Magnification from Composite Sample Molded using a) Hot Compaction b) Extrusion Method

Voids are frequently observed at the grain boundaries of large-sized microcarbon particles, while the carbon-rich interphase area is not notably significant for extruded samples. These interphase constituents significantly enhance composites' electrical conductivity [6].

Data analysis from microstructure observations and SEM EDX suggests that the composite sample achieves optimal dispersion of microcarbon. However, the micro carbon content is lower than that of the hot compaction composite sample. The extruded composite sample is less conductive than the hot compaction composite sample to be confirmed.

This article discusses observations of composite samples from different extruder head zones. Electrical conductivity decreased in samples after extrusion to the relaxation zone, Z3, the observations were limited to this zone. SEM EDX observations revealed differences in micro carbon dispersion and void presence between extrusion-printed and hot compaction samples. As seen in the SEM EDX observations, Figure 9 illustrates the microstructure observed at a 100× magnification using the Backscattered Electron/BSE method. Voids in extrusion-printed samples are observed parallel to grain boundaries, indicating potential differences in fluid layer characteristics due to compression energy during extrusion.

Cracks in the form of longitudinal grooves are thought to be a form of flow resistance from a mixture of carbon particles and LLDPE. Cavities or porous cavities indicate the presence of air trapped in the composite during the printing process, as shown in Figure 9 (a). Figure 9 (b) shows the direction of plastic flow in the molding process, and the cracks show the rheological resistance of the flow of the carbon-LLDPE particle mixture. Figure 10, conducted at 2000× Magnification, provides a more detailed examination of the voids. A particle agglomeration under 2μm found in Figure 10.

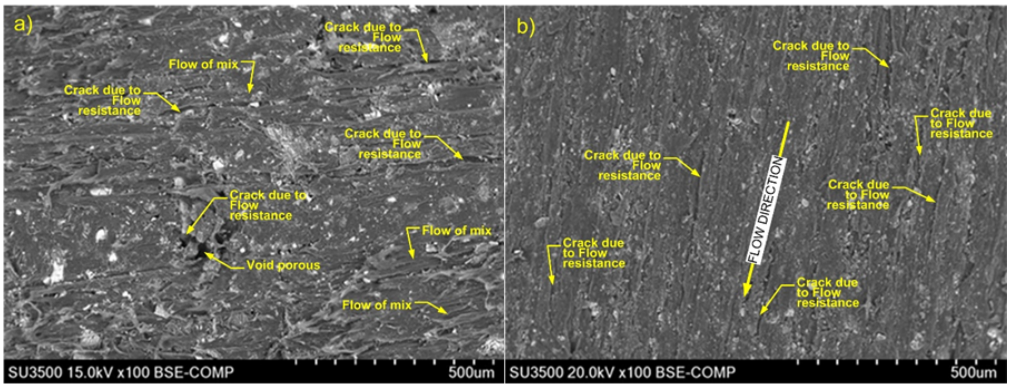

Figure 9. Micro Structure in zona 3 of extruder head chamber

a) Hot Compaction b) Extrusion Process

In the interphase area, silica impurity particles are also visible, indicating the presence of small-sized silica particles within the composite, although carbon particles are generally more dominant. Large voids around these agglomerations support the hypothesis that the dimensions of the particles influence the interaction between filler particles and the polymer [7]. The percolation threshold excludes the influence of the carbon structure as filler in conductive composites [20]. Its crystal structure closely resembles micro-sized carbon [20]. The particle size of microcarbon can impact its dispersion within the composite, with finer filler materials resulting in enhanced dispersion [7].

3. 4 Extruder Head Elaboration

Before conducting an experimental composite extrusion process, a simulation model was developed using SW software to analyze the behavior of pure virgin LLDPE. The simulation hinged on the use of recorded data in Table 3, related to the energy generated by screw rotation, with the primary goal to deduce the volumetric flow rate of the composite material [10]. The simulation aimed to approach pressure and temperature behavior during the extrusion of LLDPE material. Thus, insights into LLDPE's response under extrusion conditions are graphically illustrated, utilizing collected experimental data shown in Figure 11.

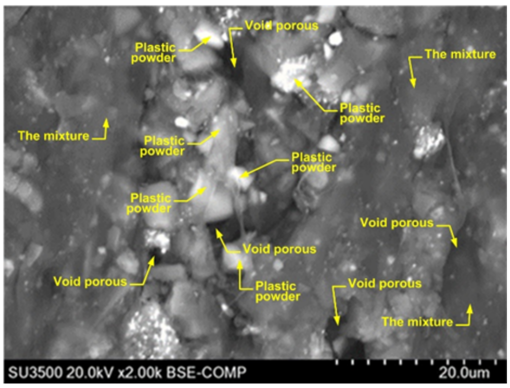

Figure 10. Microstructure of Agglomeration Point

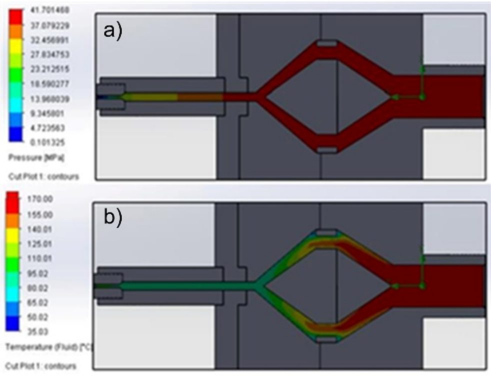

Figure 11. Profile of a) Pressure and b) Temperature of Virgin LLDPE Material Extrusion

A non-Newtonian model for LLDPE was generated using SW software. It has constant density and no pressure loss during extrusion, behaving as an incompressible fluid. Contrary to the experiment, a composite material containing 50% microcarbon from rice husk depicted a material burst at the nozzle's tip.

The designated extruder head shown in Figure 11 indicated a non-Newtonian fluid of LLDPE material. Real-time pressure measurements during the extrusion process were not feasible to compare with the pressure profiles generated by the simulation at the time. Consequently, exclusive reliance was placed on the simulation results depicted in Figure 11b to estimate the necessary temperature adjustments at the extruder head for maintaining a consistent density throughout the extrusion process as a reference.

Temperature adjustments were manually set up to achieve optimal natural temperature at the nozzle tip (110°C), aiming for consistent density without relying on a cooling machine. This kept the nozzle tip cooler than the Z1 extruder head. These settings would benefit the gradual pressure of Figure 11. SEM EDX observations revealed the presence of fluid layering, indicating the occurrence of a laminar flow in the molten composite, as shown in Figure 12.

3. 5 Electrical Resistance

The measurement of the extruded composite samples revealed an average electrical resistance in the affected zones, as illustrated in Figure 13. The TCP method addressed the challenging geometric shape, which is difficult to prepare according to the standard Four Point Probe (FPP) sample measurement. A significant deviation in data was observed within zone Z1, indicating a variation in carbon concentration within the composite samples prepared from this chamber.

It is suspected that in chamber Z1, there is still turbulent flow coming from the barrel due to the insignificant difference in the cross-sectional area [9]. This condition persists in zone Z2, which represents the initial relaxation phase of the extrusion process, indicated in Figure 11.

Table 3. Measured Data of Screw and Barrel

Parameter of Screw and Barrel:	Symbol	Value	Unit
Screw Diameter	D	26,3	mm
Pitch	t	30	mm
Actual Channel Depth	h_1	5	mm
Channel Depth (0.2 * D)	h	5,26	mm
Number of Channel	m	1	mm
Ridge Width	e	3,16	mm
Screw Length	L	490	mm
Actual Fillet Clearance	δ_1	0,15	mm
Fillet Clearance (0.002 * D)	δ	0,0532	mm
Helix Angle	ϕ	19,95	°
Cosine ϕ	Cos ϕ	0,4549	
Square Cosine ϕ	$\text{Cos}^2\ \phi$	0,2069	
Nozzle Diameter	d	20	mm
Nozzle Length	L_z	10	mm
Barrel Temperature	T_B	160	°C
Barrel Diameter (Inner)	D_B	26,6	mm

The electrical resistance was higher in these zones than in the other zones. The decrease in electrical resistance was particularly noticeable in zone Z3, a chamber equipped with a spider-leg channel designed to induce the transition from turbulent to laminar flow. Figure 12 shows layer stacking from compounding processes consisting of voids at layer intersections. A stable composite density and low electrical resistance were achieved, indicating success for the extruder head prototype [7]. A thorough analysis of the microstructure across the zone can provide insights into microcarbon particle dispersion and layer distribution during extrusions. These observations can validate conductivity enhancement by electrical resistance reduction. The spider leg successfully facilitated the extrusion of high-loading microcarbon composites, reaching up to 50% loading.

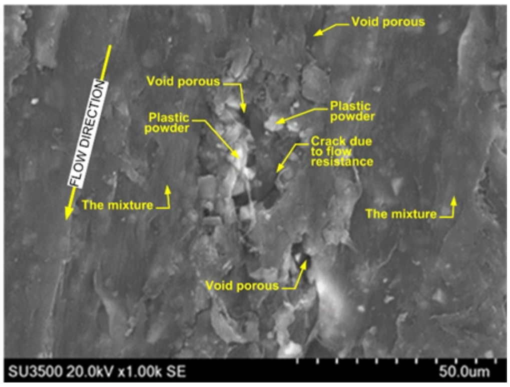

Figure 12. Laminar Pattern of Fluid Layering in Z3

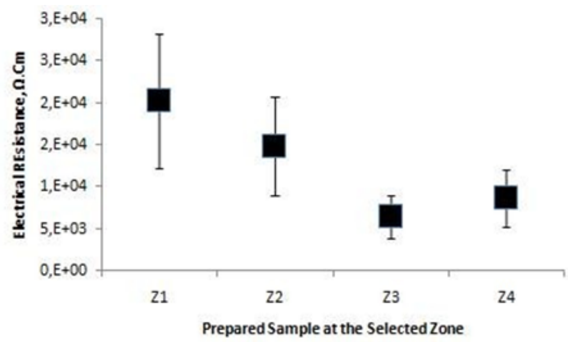

Figure 13. Electrical Resistance at each zone

4. Conclusion

A fifty-fifty loading ratio of LLDPE polymer and micro carbon particles derived from rice husk composites were stabilized using auxiliary tools designated for a single screw extrusion machine. It was determined that an extrusion temperature of 110°C at the extruder head was optimal for the composite material, resulting in a stabilized density of approximately 1 g/cm^3. Electrical conductivity measurements were performed using the Two Contact Probe method, demonstrating a notable increase in conductivity within the relaxation zone featuring a spider-leg structure. A significant reduction in resistivity was observed within the relaxation zone (Z3), which was consistently maintained at the order of 10^3 ohms within the compression zone (Z4). However, voids were detected in the composite through microstructure observation, which was noted at the laminar pattern of the composite layer. The extruded composite sample exhibits a reduction in interphase areas enriched with smaller carbon particles compared to the hot compacted composites. These findings underscore the successful development of a CPC material with improved electrical conductivity, making it a highly suitable tool for high carbon-loading composite material.

Acknowledgments : The author thanks the Research and Community Service Unit of Politeknik Negeri Jakarta for funding the research. The research was funded through the Higher Education Leading Vocational Product Research Scheme 2023 (PMTA Program), contract number 179/PL3.18/PT.00.01/2023, Politeknik Negeri Jakarta.
The authors acknowledge the facilities, scientific and technical support from Advanced Characterization Laboratories, National Research and Innovation Agency through E-Layanan Sains, Badan Riset dan Inovasi Nasional (BRIN), Serpong, Indonesia.

Conflicts of Interest: "The authors declare no conflict of interest."

References

1. Younes, H., Christensen, G., Groven, L., Hong, H. & Smith, P. Three dimensional (3D) percolation network structure: Key to form stable carbon nano grease. *J. Appl. Res. Technol.* **14**, 375–382 (2016).
2. Zuhri, A., Setyadi, I., Edy Pramono, A. & Mustofa Kamal, D. Stabilisasi Densitas Filamen dari Komposit LLDPE-Karbon Mikro melalui Rancang Bangun Kanal Spider Leg. *J. Mek. Terap.* **4**, 69–77 (2023).
3. Pötschke, P. *et al.* Melt mixing as method to disperse carbon nanotubes into thermoplastic polymers. *Fullerenes Nanotub. Carbon Nanostructures* **13**, 211–224 (2005).
4. Kwok, S. W. *et al.* Electrically conductive filament for 3D-printed circuits and sensors. *Appl. Mater. Today* **9**, 167–175 (2017).
5. Yuan, Q., Bateman, S. A. & Wu, D. Mechanical and conductive properties of carbon black-filled high-density polyethylene, low-density polyethylene, and linear low-density polyethylene. *J. Thermoplast. Compos. Mater.* **23**, 459–471 (2010).
6. Banerjee, J. & Dutta, K. Melt-mixed carbon nanotubes/polymer nanocomposites. *Polym. Compos.* **40**, 4473–4488 (2019).
7. Zuhri, A., Pramono, A. E., Setyadi, I., Maksum, A. & Indayaningsih, N. Effect of microcarbon particle size and dispersion on the electrical conductivity of LLDPE-carbon composite. *J. Appl. Res. Technol.* **13**, 374–381 (2024).
8. Al-Salem, S. M. *et al.* Effect of Die Head Temperature at Compounding Stage on the Degradation of Linear Low Density Polyethylene/Plastic Film Waste Blends after Accelerated Weathering. *Int. J. Polym. Sci.* **2016**, 8–11 (2016).
9. Kouzilos, G. N., Seretis, G. V., Provatidis, C. G. & Manolakos, D. E. Design of Polymer Extrusion Dies Using Finite Element Analysis. *Extrus. Met. Polym. Food Prod.* (2018) doi:10.5772/intechopen.72211.

10. Münstedt, H. & Starý, Z. Is electrical percolation in carbon-filled polymers reflected by rheological properties? *Polymer (Guildf).* **98**, 51–60 (2016).
11. Yousefi, N., Fisher, S. J., Burgstaller, C., Shaffer, M. S. P. & Bismarck, A. Hierarchical carbon fibre composites incorporating high loadings of carbon nanotubes. *Compos. Sci. Technol.* **222**, 109369 (2022).
12. Djafar, A. & Fatoni, M. A. Perancangan Mesin Single Screw Extruder Untuk Daur Ulang Plastik Ldpe Menjadi Filament Feed 3D Printing. *J. Ilm. Teknol. dan Rekayasa* **26**, 205–217 (2021).
13. Pramono, A. E., Ruswanto, S. & Indayaningsih, N. Effect of pyrolysis sintering temperature on the electrical current delivery power of kaolin-carbon composites. *J. Ceram. Process. Res.* **23**, 171–180 (2022).
14. Madsen, B. & Lilholt, H. Physical and mechanical properties of unidirectional plant fibre composites-an evaluation of the influence of porosity. *Compos. Sci. Technol.* **63**, 1265–1272 (2003).
15. Yang, Y. *et al.* High performance carbon-based planar perovskite solar cells by hot-pressing approach. *Sol. Energy Mater. Sol. Cells* **210**, 110517 (2020).
16. Sun, L., Park, S. S., Sheberla, D. & Dincă, M. Measuring and Reporting Electrical Conductivity in Metal-Organic Frameworks: Cd2(TTFTB) as a Case Study. *J. Am. Chem. Soc.* **138**, 14772–14782 (2016).
17. Pramono, A. E., Rahman, H., Adhi, P. M. & Indayaningsih, N. Controlling the size and carbon composition to determine the electrical conductivity of the kaolin-carbon composite. *J. Ceram. Process. Res.* **23**, 638–646 (2022).
18. Jørgensen, J. K., Larsen, Å. & Helland, I. Study on LLDPE molecular structure characterization by preparative and analytical cross-fractionation. *E-Polymers* (2010) doi:10.1515/epoly.2010.10.1.1596.
19. Maksum, A., Rustandi, A., Permana, S. & Soedarsono, J. W. Roasting-quenching pretreatment in the calcination process to improve the purity of rice husk bio-silica. *JP J. Heat Mass Transf.* **16**, 313–326 (2019).
20. Balberg, I. A comprehensive picture of the electrical phenomena in carbon black-polymer composites. *Carbon N. Y.* **40**, 139–143 (2002).